SIMULATION OF ANTAGONISTIC MUSCLE ACTIONS THROUGH THE USE OF SLIDING-MODE CONTROL TECHNIQUES

S.J. Lister * **S.K. Spurgeon** * **J.J.A. Scott** ** **N.B. Jones** *

* *The Department of Engineering, The University of Leicester, LE1 7RH, UK*
** *The Department of Pre-Clinical Sciences, The University of Leicester, LE1 7RH, UK*

Abstract: A sliding-mode controller is applied to a two-dimensional, ten-segment human locomotor system model in order to track kinematic gait samples. Motion tracking is performed to within 2 degrees of the references for the mean of ten samples with driving moments typically within two standard deviations of the expected values. The use of sliding-mode techniques also produces antagonistic muscle activity at periods similar to those measured from experimental subjects.

Keywords: Biomedical control, Sliding-mode, Human Walking Simulation

1. INTRODUCTION

Human locomotor system models are an increasingly common way of studying gait and many have been developed in recent years (Zajac *et al.*, 2002; Zajac *et al.*, 2003). The application of control techniques increases the versatility of these models, permitting more detailed study of the processes involved in gait as well as the development of FES (Functional Electrical Stimulation) based therapies for pathological conditions.

Where control models do exist they are typically based around the knee (Ferrarin *et al.*, 2001; Jezernik *et al.*, 2004; Lim *et al.*, 2003; Schauer *et al.*, 2003) or ankle joints if not individual muscles (Negrd *et al.*, 2003; Watanabe *et al.*, 1999). Larger models tend to be concerned only with paraplegia or robotics (Davoodi *et al.*, n.d.; Ephanov and Hurmuzlu, 1997; Popovic *et al.*, 1999; Riener and Fuhr, 1998). For this study a model was developed to simulate both normal gait and relatively minor pathological locomotion patterns. It comprises 2-dimensional simulation of the human locomotor system composed of 10 rigid segments (upper body, pelvis, thighs, shanks, feet and toes) developed using Lagrange's equations and a total of 50 musculotendon actuators grouped according to their influence on the joints. Ligaments at the hips and knees were also included to prevent hyperextension of these joints.

A sliding-mode controller was applied to drive the model to follow measured gait trajectories. The attraction of sliding-mode control is based on its order reduction properties and its insensitivity to certain types of uncertainty (Edwards and Spurgeon, 1998), which permits precise tracking of model to subject even with such complex nonlinear systems as the human body. It was for these reasons that it was decided to begin an investigation into the value of sliding-mode techniques for human motion control as an alternative to the commonly used control strategies.

During this early model development it was seen that the motion tracking controller immediately began to produce antagonism (simultaneous contraction of opposing muscles) in the muscle activity patterns as a result of its switching function. This was not a designed property, but found to be an unexpected benefit of the sliding-mode approach.

Sections 2 and 3 briefly describe the human neuromusculoskeletal model and the application of a sliding-mode controller to drive it. The motion tracking, joint moment and muscle activity results for a set of normal individuals are then presented in Section 4.

2. THE MODEL

Due to space limitations, the full details of the model cannot be included here. The following is only an overview.

A two-dimensional ten-segment pin-jointed model (see Figure 1) was used to simulate human gait patterns, the motion dynamics developed using Lagrange's equations and described by the equation:

$$a = M^{-1} f \tag{1}$$

Where a is a vector of linear and angular accelerations of the body segments, f is a vector of the forces and moments acting on the body and M is a 12*12 mass and moment of inertia matrix.

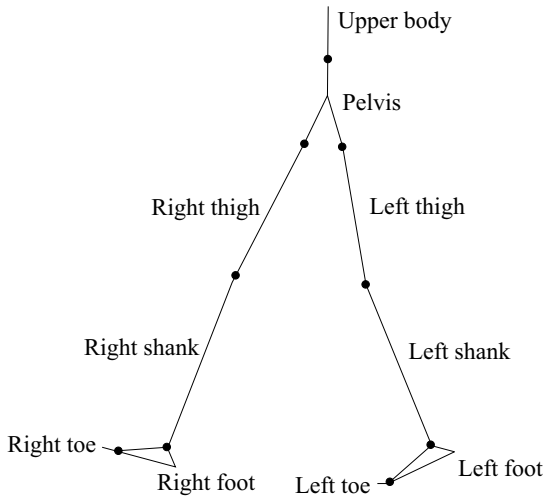

Fig. 1. Stick figure of the body segments.

Data from sources of cadaver measurements were used to provide the set of default body segment parameters used in the model (Delp, 1990; Larivire and Gagnon, 1999; Piazza and Delp, 1996). Hyperextension ligaments at the hip and knee joints were modelled using equations from Piazza and Delp ((Piazza and Delp, 1996)).

A modified Hill-type musculotendon actuator model as seen in Figure 2 describes the force produced by each muscle based on the level of activation and the length and contraction velocity conditions. Full details of this muscle model can be found in publications of Zajac and Delp (Delp, 1990; Delp and Zajac, 1992; Piazza and Delp, 1996; Zajac, 1989; Zajac and Stevenson, 1986).

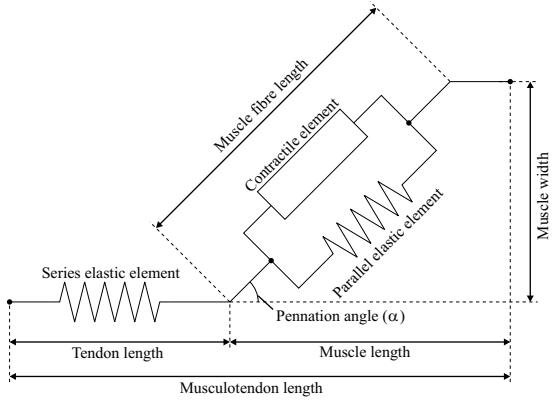

Fig. 2. Hill-type musculotendon model.

Parameters for the musculotendon actuators describing all of the significant muscles in the right leg for a generic, normal individual were obtained from the International Society of Biomechanics website (Delp, 1990) (for the left leg of the model, the muscle parameters used in the right leg are reflected). Geometrical calculations based on the relative positions of the muscle attachment sites to the joints were then used to find the influence of the muscles on the body.

The muscles were grouped on each side for practical purposes according to their actions across the joints: lumbar flexors, lumbar extensors, hip flexors, hip extensors, hip & knee flexors, hip & knee extensors, knee flexor, knee extensors, knee & ankle flexors, ankle plantarflexor, ankle dorsiflexor, ankle plantarflexors & toe flexors, ankle dorsiflexors & toe extensors. It should be noted that reference data was not available for all of these groups for comparison in the results section.

Ground reactions for the model were produced by applying the force plate readings to the foot segments. This is by no means an ideal solution, however the authors have been unable to find or generate a model which produces ground reactions sufficiently similar to those measured in practice.

3. SLIDING-MODE CONTROLLER

A modified control law from Edwards & Spurgeon (Edwards and Spurgeon, 1998) pp. 11-15, including a linear feedback component to provide asymptotic reaching of the sliding surface, was applied to the model:

$$u(t) = \ddot{e} - (\lambda + \Phi)\dot{e}(t) - \Phi\lambda e(t) - \rho sgn(s(t)) \tag{2}$$

Where u is the system input, e is the error in the segment angle, λ is a positive design scalar defining the switching function:

$$s = \lambda e + \dot{e} \tag{3}$$

The control objective is to force s to zero and attain the sliding mode. Φ is a positive design scalar introduced to prescribe an asymptotically stable first order dynamic to the error signal and thus permit a reduction in ρ, a positive design scalar defining the switching amplitude.

For simulation purposes there were no physical constraints on the controller gain, so the following parameter values were chosen on the basis that they provided rapid error decay and maintained sliding motion across the gait cycle:

$$\lambda = 200 \tag{4}$$

$$\rho = 200 \tag{5}$$

$$\Phi = 100 \tag{6}$$

Sliding-mode techniques produce a reduction to a first-order decay regardless of the complexity of the second-order plant being controlled, which continues for as long as the control action is powerful enough to maintain the sliding-motion. The controller also cancels the effects of disturbances in the closed loop system without requiring any knowledge of those disturbances. This insensitivity to unmodelled dynamics and parameter inaccuracies gives sliding-mode techniques an advantage in the control of simulated human motion.

For the human locomotor model under consideration here, assume a set of desired reference signals; x_{ref}, $\dot{x}_{ref}$ and $\ddot{x}_{ref}$, are available from measured kinematic data. The error between the measured data and model outputs (x_{sim}, $\dot{x}_{sim}$) can be defined as:

$$e = x_{sim} - x_{ref} \tag{7}$$

$$\dot{e} = \dot{x}_{sim} - \dot{x}_{ref} \tag{8}$$

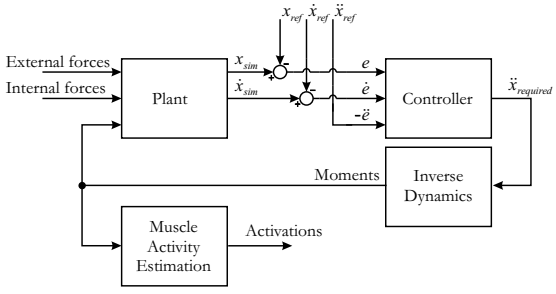

Fig. 3. Block diagram of controlled system. The external forces acting on the plant include ground reactions and gravity. The internal forces are ligament and passive muscular forces. The controlling moments represent the active muscle behaviour.

$$\ddot{e} = -\ddot{x}_{ref} \tag{9}$$

The output from the controller is then a set of desired accelerations ($\ddot{x}_{desired}$), which must be passed through the mass and moment of inertia matrix of equation (1) in order to generate the moments required to drive the model (Figure 3).

For simplicity at this early stage of development, the moments from the controller were used to drive the model segments directly with muscle activity estimated independently under open-loop conditions (see Figure 3).

Using the Hill-type model, muscle activity can be calculated at each instant by dividing the control moment, T_c, by the maximum moment that the muscle can generate about the joint at that instant, T_{max}:

$$activation = \begin{cases} \dfrac{T_c}{T_{max}}, & for\ \dfrac{T_c}{T_{max}} > 0 \\ 0, & for\ \dfrac{T_c}{T_{max}} < 0 \end{cases} \tag{10}$$

The activation signals are constrained to be greater than zero, so control moments must be distributed between the muscles of antagonistic pairs (muscles on opposite sides of a joint). (N.B. using this muscle model, activity (not neural excitation) is linear with the maximum instantaneous muscle force (not maximum isometric muscle force))

Only one pair of antagonistic muscle groups cross the toe joints, providing a straight-forward calculation. These muscles also cross the ankle and the result of any activation must be calculated for this joint before finding the activations of the other muscle groups crossing the ankle.

Soleus and gastrocnemius oppose tibialis anterior across the ankle, but gastrocnemius also crosses the knee joint. Therefore the distribution of activity between soleus and gastrocnemius is chosen to minimise the knee moment whilst still completely accounting for the ankle moment, i.e. for a plantarflexion moment across the ankle:

$$\begin{aligned} T_{ankle} =& A_{soleus} \times T_{max\_soleus\_ankle} \\ &+ A_{gastroc} \times T_{max\_gastroc\_ankle} \end{aligned} \tag{11}$$

where:

$$T_{knee\_min} = |T_{knee} - T_{max\_gastroc\_knee} A_{gastroc}| \tag{12}$$

$T_{(.)}$ represents the moment about the stated joint as either the moment required to be accounted for or the maximum that can be generated by the muscle stated. $A_{(.)}$ is the level of activation of the stated muscle.

As there are only three remaining antagonistic muscle group pairs crossing the hip and knee joints it is possible to calculate each of the six possible minimum activity distributions and select the smallest. Only one pair crosses the lumbar joint.

In order to produce a more realistic outcome, an additional constraint ensures that muscles performing similar actions cannot be activated excessively higher than each other:

$$|A_1^2 - A_2^2| \leq 0.25 \tag{13}$$

This constraint is not devised based on quantitative measurement of the relationships between muscle actions, but is rather a rendering of the intuitive fact that large loads are distributed between suitable muscles.

4. RESULTS

Figure 4 demonstrates the average motion tracking results for ten gait samples. Joint angles are represented, rather than the segment angles calculated directly by the model, as they are more appropriate for gait analysis. To avoid settling time issues, the gait cycle is repeated with the end-start transition between cycles interpolated for a few frames and only the second cycle is shown.

Sub-figures (d), (e) and (f) of Figure 4 show the moments required to drive the model to follow the reference trajectories in (a), (b) and (c). The mean reference moments and standard deviations to either side of it are included for comparison. These reference curves were included in the original data files and were calculated using the software the data was sampled and processed with.

In the absence of EMG (electromyogram) data for all of the data sets used in this study, simulated muscle activity is compared to normal activity approximations from Perry (Perry, 1992) in Figure 5. An exact match cannot be expected under these circumstances, but some idea of the model's performance can be obtained. The bars represent the periods where the EMG and activation curves rise above the mean level for those muscles during the cycle. This is a common method of assessing the performance of muscle activity estimators and measuring the correlation between EMG signals and simulated muscle activity (Lu, 1999; Nordin and Frankel, 2001; Zajac *et al.*, 2002; Zajac *et al.*, 2003).

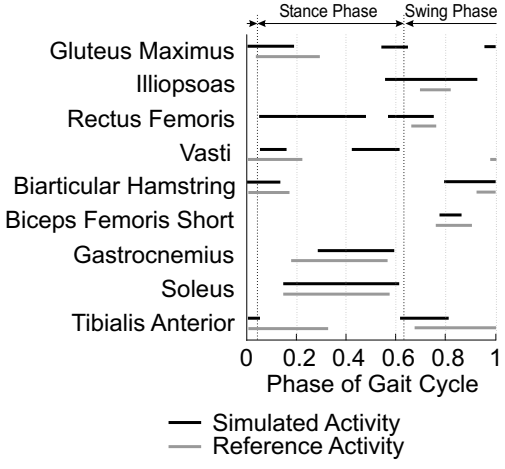

Fig. 5. Average simulated leg muscle activity compared to approximate data from Perry.

5. DISCUSSION

The controller provides motion tracking of the sampled gait patterns with a maximum error of 1.71 degrees from the reference trajectories, well within the one standard deviation range illustrated in Figure 4 (sub-figures a-c). The largest errors occur at maximal extension of the hip joint as the hyperextension ligaments act against the system. The gait pattern of an individual would normally take this action into account but the model operates using default parameters for which the joint angle trajectories are not optimised. Despite this the elastic, energy efficient behaviour of the hip ligaments make them a useful component of the model.

The joint moments (Figure 4 (d-f)) show much greater variation from the reference signals, especially in the swing phase where the limb acts as a pendulum undergoing rapid acceleration and deceleration and is therefore more sensitive to parameter variations than during the more sedate and stable stance phase. Measuring a subject's physical parameters rather than using a default set would reduce the error, although without taking in vitro measurements of the joint moments, which is extremely impractical, generating closely matching data proves only that the methods of calculation were similar, not that the data are accurate.

The simulated muscle activity estimation provides a correlation of 74.8% with the reference EMG signals in measuring activity greater than average (Figure 5), which is consistent with other work in the field (Lu, 1999; Zajac *et al.*, 2002; Zajac *et al.*, 2003). Differences that occur suggest unmodelled joint dynamics and inaccuracies in the muscle parameters. The error in joint moments (Figure 4 (d-f)) could also account for some of the differences, although similar moments prove only that the methods of calculation were similar, not that the results are accurate.

The most significant deviation of muscle activity is seen in the rectus femoris muscle. It is consistently stimulated far more than the reference suggesting that the muscle geometry makes it a more desirable choice for activation than is the case in practice. However, taking accurate parametric readings for every muscle and ligament within the body would be more difficult and time consuming than measuring EMG readings directly.

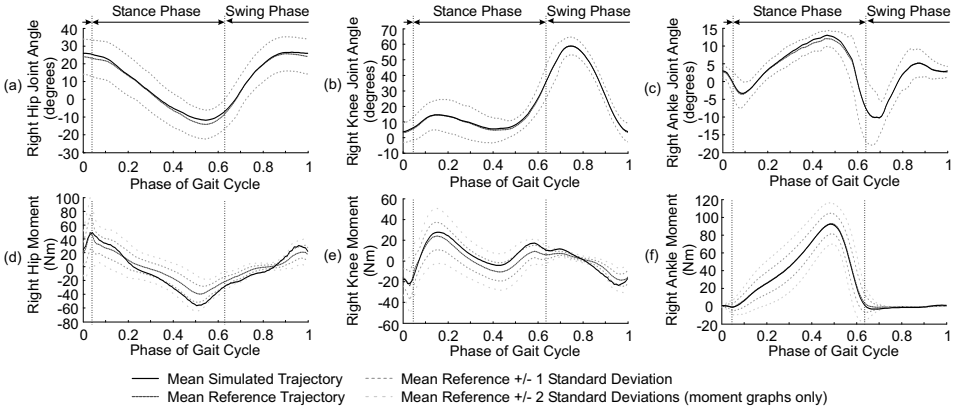

Fig. 4. Average joint angle and moment motion tracking results for the right leg

Significantly, antagonism can be seen in the activity of the muscles crossing the hip and knee joints. Gluteus maximus and the biarticular hamstrings act in opposition across the hip to iliopsoas and rectus femoris while the hamstrings oppose the vasti and rectus femoris across the knee. However there are periods where opposing muscles are activated simultaneously. At periods during the gait cycle the joint angles are particularly sensitive to changes in moments and antagonism occurs to stabilise the motion. Likewise the high frequency oscillation of the sliding-mode controller has a greater effect at these sensitive points, causing the stimulation of both sides of an antagonistic pair.

The gastrocnemii and soleus muscles oppose tibialis anterior across the ankle joint. However there is no antagonism seen in the simulated results while it is extensive in the reference EMG measurements. Tibialis anterior in particular shows a much reduced level of activity at the beginning of the stance phase where it would normally contract to help stabilise the joint as body weight is transferred to the limb. This suggests that the modelled ankle is more stable than the reference ankles so that the switching function of the controller does not produce an amplitude of oscillation in the moment sufficient to cross zero and thus stimulate both muscles. It was also noted that the magnitude of the simulated activity of the gastrocnemii and soleus were consistently lower than expected, meaning a smaller change in activation is required to control the moment thus reducing or eliminating the antagonism. This implies that parameter differences are again the cause.

6. CONCLUSION

Gait patterns are optimised for minimum energy consumption given the individuals physical characteristics (Anderson and Pandy, 2001). Parameters such as segment mass and length, muscle strength and geometries and ligament behaviour clearly influence this relationship between motion and energy use. Forcing the model to follow the gait pattern of a subject using only default parameters, it is almost inevitable that the joint moments and muscle actions will show discrepancies from the expected curves and that the pattern will be less than optimal for the model. In order to reduce errors, more of the physical parameters of each subject must be measured and applied to the model during simulation, although as there are several hundred required to define the model exactly some compromise must be reached.

The value of the sliding-mode techniques is the insensitivity to this sort of plant-model mismatch. It is possible to produce a control effort comparable to the human nervous system without the need for detailed knowledge of it or of the body being controlled. The emergence of antagonism is an unexpected benefit of this technique and further demonstrates the value of the control strategy in the simulation of neuromuscular control signals. Previous attempts have been made to simulate antagonism (Kaufman *et al.*, 1999), but it is an inherent feature of the sliding-mode approach.

The antagonism provided by this model is somewhat inconsistent in its occurrences; in particular the ankle joint shows no antagonism where a significant amount would normally be expected. Redesigning the controller with antagonism specifically in mind would help and greater parametric accuracy could increase the correlation between simulated and measured muscle activity, consideration should be given to reducing the strength of the modelled calf muscles at least. However, perfect accuracy cannot be expected as muscle stimulation patterns change with the physical condition of the subject and even between one step and the next. Knowledge of the neural processes involved in muscle selection and activation during motion is also very limited preventing direct duplication. Any muscle activity pattern should be considered to represent one of a myriad possibilities and providing it is capable of generating the required gait, it is just as valid as the measured one.

ACKNOWLEDGEMENTS

The authors gratefully acknowledge the support of the Leverhulme Trust to this project (Ref no. F/00212/K).

Thanks are also due to Dr Michael Barnes for his technical support and the Leicester General Hospital for the use of their motion analysis equipment during the collection of data for this project.

REFERENCES

Anderson, F.C. and M.G. Pandy (2001). Dynamic optimization of human walking. *Journal of Biomechanics* **34**(5), 381–390.

Davoodi, R., B.J. Andrews and G.D. Wheeler (n.d.). Manual and automatic control of fes-assisted indoor rowing exercise.

Delp, S.L. (1990). Parameters for a model of the lower limb. *The International Society of Biomechanics website (URL: http://isb.ri.ccf.org./data/delp/).*

Delp, S.L. and F.E. Zajac (1992). Force and moment generating capacity of lower extremity muscles before and after tendon lengthening. *Clinical Orthopaedics and Related Research* **284**, 247–259.

Edwards, C. and S.K. Spurgeon (1998). *Sliding Mode Control Theory and Applications*. Taylor and Francis LTD.

Ephanov, A. and Y. Hurmuzlu (1997). Generating pathological gait patterns via the use of robotic locomotion models.

Ferrarin, M., F. Palazzo, R. Riener and J. Quintern (2001). Model-based control of fes-induced single joint movements. *IEEE Transactions on Neural Systems and Rehabilitation Engineering* **9**(3), 245–258.

Jezernik, S., R.G.V. Wassink and T. Keller (2004). Sliding mode closed loop control of fes: Controlling the shank movement. *IEEE Transactions on Biomedical Engineering* **51**(2), 263–272.

Kaufman, K. R., E. Y. S. Chao and H. E. Rubash (1999). Predication of antagonistic muscle forces using inverse dynamic optimization during flexion/extension of the knee. *Transactions of the ASME Journal of Biomedical Engineering* **121**, 316–322.

Larivire, C. and D. Gagnon (1999). The influence of trunk modelling on 3d biomechanical analysis of simple and complex lifting tasks. *Journal of Clinical Biomechanics* **14**, 449–461.

Lim, C. L., N. B. Jones, S. K. Spurgeon and J. J. A. Scott (2003). Reconstruction of human neuromuscular control signals using a sliding mode control technique. *Simulation Modelling Practice and Theory* **11**, 223–235.

Lu, T. (1999). Muscle recruitment strategies of the human locomotor system during normal walking: A mechanical perspective. *Biomedical Engineering Applications Basis Communications* **11**, 191–202.

Negrd, N.O., T. Schauer and J. Raisch (2003). Robust nonlinear control of single limb movement. In: *Proc. of the 5th IFAC Symposium on Modelling and Control in Biomedical Systems (Including Biological Systems).*

Nordin, M. and V.H. Frankel (2001). *Basic Biomechanics of the Musculoskeletal System*. 3rd ed.. Lippincott, Williams & Wilkins.

Perry, J. (1992). *Gait Analysis*. SLACK, Thorofare, NJ.

Piazza, S.J. and S.L. Delp (1996). The influence of muscles on knee flexion during the swing phase of gait. *Journal of Biomechanics* **29**, 723–733.

Popovic, D., R.B. Stein, M.N. Oguztoreli, M. Lebiedowska and S. Jonic (1999). Optimal control of walking with functional electrical stimulation: A computer simulation study. *IEEE Transactions on Rehabilitation Engineering* **7**(1), 69–79.

Riener, R. and T. Fuhr (1998). Patient-driven control of fes-supported standing up: a simulation study. *IEEE Transaciton on Rehabilitation Engineering* **6**(2), 113–124.

Schauer, T., W. Holderbaum and K.J. Hunt (2003). Sliding-mode control of knee-joint angle: experimental results. In: *Proceedings of the International Functional Electrical Stimulation Society 2002 Conference*. pp. 316–318.

Watanabe, T., R. Futami, N. Hoshimiya and Y. Handa (1999). An approach to a muscle model with a stimulus frequency-force relationship for fes applications. *IEEE Transactions on Rehabilitation Engineering* **7**(1), 12–18.

Zajac, F.E. (1989). Muscle and tendon: Properties, models, scaling and application to biomechanics and motor control. *Critical Reviews Biomedical Engineering* **17**, 359–411.

Zajac, F.E., R. R. Neptune and S. A. Kautz (2002). Biomechanics and muscle coordination of human walking part i: Introduction to concepts, power transfer, dynamics and simulations. *Gait and Posture* **16**, 215–232.

Zajac, F.E., R. R. Neptune and S. A. Kautz (2003). Biomechanics and muscle coordination of human walking part ii: Lessons from dynamical simulations and clinical implications. *Gait and Posture* **17**, 1–17.

Zajac, F.E. Topp, E.L. and P.J. Stevenson (1986). A dimensionless musculotendon model. In: *Proceedings of the 8th Annual Conference of the Engineering in Medicine and Biology Society*. pp. 601–604.